QUANTATAIVE ANALYSIS OF RELATIONSHIP BETWEEN ALOS PALSAR BACKSCATTER AND FOREST STAND VOLUME

Choen Kim
College of Forest Science, Kookmin University, Seongbuk-gu, Seoul, Korea., choenkim@kookmin.ac.kr

QUANTATAIVE ANALYSIS OF RELATIONSHIP BETWEEN ALOS PALSAR BACKSCATTER AND FOREST STAND VOLUME

Acknowledgements

QUANTATAIVE ANALYSIS OF RELATIONSHIP BETWEEN ALOS PALSAR BACKSCATTER AND FOREST STAND VOLUME

Choen Kim

ABSTRACT

To estimate forest stand volume, topographic effects should be considered in Synthetic Aperture Radar (SAR) data processing, because most forests are located on mountainous areas in Korea. This paper shows how the effects on the ALOS Phased-Array L-Band SAR (PALSAR) backscatter in Kwangneung Experiment Forest can be reduced by gamma-nought γ^0.

Regardless of coniferous and deciduous forests, the gamma-nought γ^0 values are always lower compared to the sigma-nought σ^0 values at HH and HV polarization for 58 standwise tree volume of the fore-slope (here, the west-facing slope) and are always higher in case of far-slope (here, east-facing slope).

Comparison of the fore-slope with the far-slope, relating to the stand volume of the γ^0 and σ^0 values, demonstrates that the σ^0 values are significantly remarkable, while the γ^0 values are not. This means that the topographic normalized backscattering coefficient γ^0 can be used to estimate tree volume, independent of fore-slope and far-slope.

Though the aforementioned two backscattering coefficients of γ^0 and σ^0 indicate L-band HH and HV saturations with tree volume observed at around 310 m³ha⁻¹, they increase with increasing trend with forest stand volume.

These results show that stand volume retrieval of mountain forests can be improved by using topographic normalized backscattering coefficient of ALOS PALSAR data.

I. INTRODUCTION

Many studies on the use of SAR data for forest biomass estimation have already presented in the literatures [1, 3, 5, 6,

9, 15]. However, they concentrated on almost flat terrain because of topography-induced backscattering variations in areas of sloped terrain [2, 14].

For this reason, recent investigations have attempted in evaluating the relationships between SAR backscatter and forest biomass in mountainous areas [4, 8, 10, 13].

The results obtained by applying the topographic normalized backscattering coefficient γ^0 from the above investigations have proven its compensation of topographic effects on the backscatter in estimating tree volume or forest biomass.

In the practical aspect regarding forest inventory, forest biomass estimates have been undertaken through the conversion of tree volume into tree biomass. Therefore, the proposed approach in this paper can also rely on retrieving forest biomass estimates at stand levels on sloping terrain.

Despite the variations of PALSAR backscattering coefficient σ^0, in case of flat and sloping forests, depending on various biophysical parameters [8, 10, 11, 13], the main purpose of this paper is to verify the remained topographic effects with respect to variations of the derived topographic normalized backscattering coefficients γ^0_{HH} and γ^0_{HV}, based on forest stand volume between the fore-slope and the far-slope.

II. STUDY AREA AND DATA

The test site is situated in 1109 ha Kwangneung Experiment Forest (KEF, Korea), 65 stands with growing stock volume in the range 112-467 m³ ha⁻¹, 127⁰9'17" - 127⁰12'05" North in latitude and 37⁰70'50" - 37⁰81'32" East in longitude, 39 km east of Seoul (see Fig. 1). The ground elevation varies from 57 to 617 m above sea level.

Vegetation of the stands characterized by brown forest soil and temperate climate is composed of coniferous, deciduous, and mixed forests. 58 stands selected for the comparison of conifers and broadleaved tree stands using gamma-nought consist of two pine species (i.e., Korean Pine and Japanese Red Pine) and two dominated deciduous species (i.e., Konara Oak and Red-leaved Hornbeam), while the 7 nonselective stands are mixed species forests.

The data of forest stand volume were collected from 2008 to 2010.

Table 1. Characteristics of the used 3 ALOS PALSAR data over the test site.

Imaging Configuration	Polarization (Chip bandwidth 14 MHz)	Incidence angle at scene center (deg)	Spatial resolution Azimuth/Range (m)
*FBD34	HH, HV	38.7	12.5/12.5

* FBD34: Fine-beam dual-polarization made with look angle (i.e., nadir-off angle) of 34.3^0.
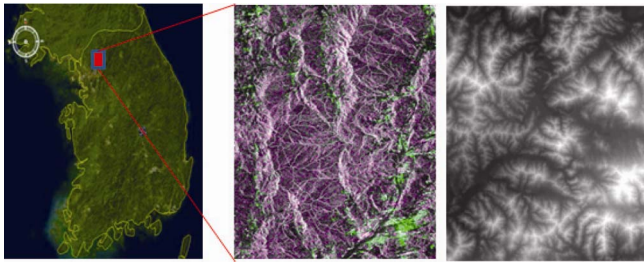

Fig. 1. ALOS PALSAR FBD34 composite of HH/HV/HV, image data acquired on March 20, 2007 over KEF study area overlaid with forest stand boundaries (center), DEM data (right).

To detect backscatter variations in phonological canopy conditions, the ALOS PALSAR level 1.5 data over the test site KEF were obtained on 20 March 2007, 29 August 2007, and 29 February 2008 respectively. Important specifications of the PALSAR data are shown in Table 1.

The level 1.5 data provided by JAXA Earth Observation Research Center(EORC) have already been preprocessed, such as radiometric and geometric corrections after range and multi-look azimuth compression (i.e., 8 looks in azimuth and 2 in range).

However, as the test site has topographic relief with steep mountain, the above geo-referened PALSAR images, without considering the altitude, need the orthorectification using a high-resolution digital elevation model (DEM) [7, 11].

The orthorecification process using 30 m DEM of National Geographic Information Institute was undertaken by means of the commercial software SARscape.

According to the conversion formula [12] with the calibration factor (CF) of -83 also in this paper, the orthorecified PALSAR images were converted to the σ^0 format, namely the normalized radar cross section (NRCS) in decibel (dB).

Then, the orthorecified sigma-nought images were transformed to the γ^0 format using the 30 m DEM-assisted topographic illumination correction algorithm [2, 14, 16], which is described in the section III.

III. METHODOLOGY

The reason for using the so called topographic normalized backscattering coefficient γ^0 is due to the fact that fore-slopes appear brighter and far-slopes appear darker in the PALSAR σ^0 images [10, 16]. To generate the PALSAR γ^0 images, the topographic illumination correction is performed by using the cosine of surface tilt angles [2, 14, 16].

The used model outlined by Thiel *et al.* [13] and Santoro *et al.* [10] is simply written as

$$\gamma^0 = \sigma^0 \frac{A_{flat}}{A_{slope}} \left(\frac{\cos \theta_{ref}}{\cos \theta_{loc}} \right)^n$$

where γ^0, σ^0 denote the topographic normalized backscattering coefficient and the (linear) backscattering coefficient, A_{flat}, A_{slope}, denote the PALSAR pixel size for a theoretical flat terrain and the true local PALSAR pixel size for the mountain terrain, and θ_{ref}, θ_{loc}, denote the incident angle (in case of this paper, 38.7^0; the incident angle at scene center) for the flat terrain and the actual local incident angle for the mountain terrain, respectively.

Theoretically, the exponent *n* can be estimated for the PALSAR backscatter and different growth stages (i.e., the optical canopy depth) of the test site. But *n* with its intervals between 0 and 1, as with [8, 10, 13], is set to 1 because the optical canopy depth is difficult to obtain in practice.

Stand-based growing stock volume instead of plot-based biomass estimates has the advantage for applying PALSAR backscatter variations between fore-slopes and far-slopes with respect to the same tree volume of even-aged pure stands separately without regarding the characteristics of forest species.

IV. RESULTS AND ANALYSIS

Results after performing the topographic illumination correction on the PALSAR images are shown in Fig. 2 as comparative regressions between γ^0 and σ^0 values (included HH and HV polarizations) depending the stand volume and the cosine of surface tilt angles.

Obviously, in the fore-slope (here, west-facing slope) corresponding to the tilted surface toward the PALSAR sensor, the relationship between the backscattering coefficient σ^0 and the stand volume (equivalent to a linear regression between σ^0 and the logarithm of tree volume) shows always lower correlation, with more RMSE, than the relationship between the topographic normalized backscattering coefficient γ^0 and the stand volume (see the left sides of Fig. 2).

In case of the far-slope (here, east-facing slope) corresponding to the tilted surface opposite to the PALSAR sensor, the former shows also always lower correlation with more RMSE than the latter (see the right sides of Fig. 2).

In addition, both the higher σ^0 values than the γ^0 values in fore-slope and the lower σ^0 values than the γ^0 values in far-slope, on the same tree volume, regardless of coniferous and deciduous forest including HH and HV polarizations, are clearly explained because topographic effects induce
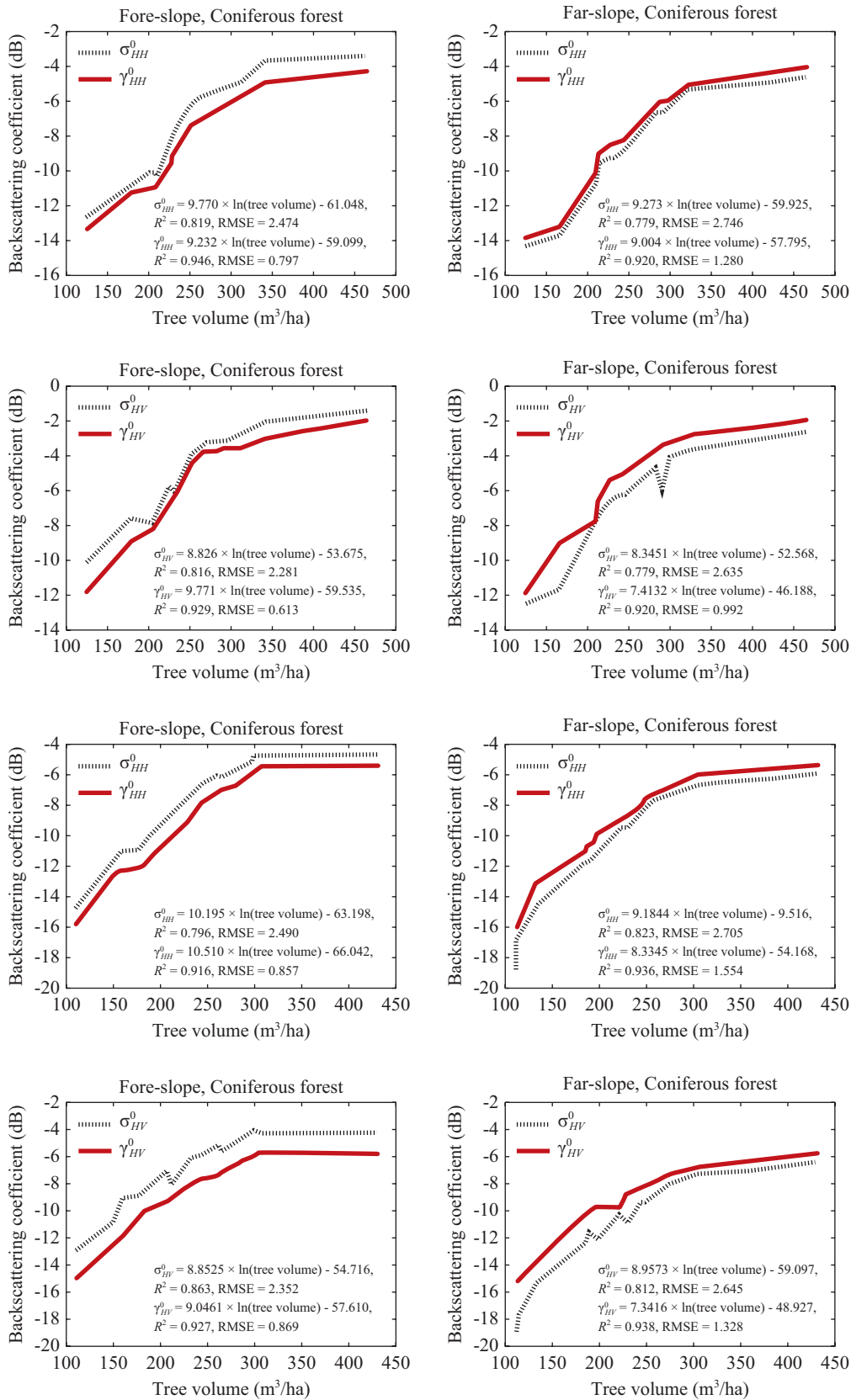
Fig. 2. Comparison of γ^0_{HH}, γ^0_{HV} with σ^0_{HH}, σ^0_{HV} between fore-slope (west-facing slope, left) and far-slope (east-facing slope, right) for tree volume in coniferous and deciduous stands derived from the 3 ALOS PALSAR images over Kwangneung Experiment Forest, Korea. The images were acquired on 20 March 2007, 29 August 2007, and 29 February 2008.

Table 1. Thet-statistic showing no difference of γ^0 and significant of σ^0 between fore-slope and far-slope, respectively.

		γ^0	σ^0
L-HH, Coniferous forest	degree of freedom	24	24
	critical value	1.711	1.711
	t-statistic	1.001	2.191
L-HV, Coniferous forest	degree of freedom	24	24
	critical value	1.711	1.711
	t-statistic	1.306	2.01
L-HH, Deciduous forest	degree of freedom	30	30
	critical value	1.697	1.697
	t-statistic	0.185	2.362
L-HV, Deciduous forest	degree of freedom	30	30
	critical value	1.697	1.697
	t-statistic	0.520	2.964

backscatter variations, in spite of the performed terrain radiometric correction using the SARscape.

In comparison with the fore-slope appearing brighter aspect and the far-slope appearing darker aspect, all the σ^0 values of the fore-slope are much higher than those of the far-slope. Such σ^0 differences related topographic effects are also verified at the significant *t*-statistic indicated in Table 2.

On the other hand, the whole γ^0 values of the fore-slope are similar to those of the far-slope and the rejected differences among the γ^0 values are much smaller in relation to the *t*-statistic listed in Table 2.

Then, it follows that application of the topographic normalized backscattering coefficient γ^0 to the PALSAR images over mountainous forest is useful for correcting not only the overestimated tree volume on fore-slope but also the underestimated one on far-slope.

For other comparisons of HH and HV polarizations, obvious differences (i.e., the average of 2.13 dB for fore-slope and of 2.66 dB for far-slope) between γ^0_{HH} and γ^0_{HV} regressions occur only in coniferous forest, independent of fore-slope and far-slope. Such differences may be explained by the influence of multiple (or strong dihedral) scattering, because all the correlation between the stand volume of γ^0_{HH} and γ^0_{HV} respectively are very high ($R^2 > 0.91$, see Fig. 2).

Finally, the saturation levels of all 8 regressions between γ^0 and the logarithm of tree volume are defined by the saturation criteria at 0.024 dB m^{3}ha^{-1} corresponding to about 310 m^{3}ha^{-1}.

V. CONCLUSION

ALOS PALSAR can generally estimate forest biomass better than shorter SAR wavelengths, because the long wavelengths of L-band penetrate the canopy, especially foliage and interact with the trunk.

But the relationship between SAR backscatter and tree volume for estimating forest biomass has mainly been investigated in various forest types only on flat and horizontal areas. This paper presents therefore the PALSAR data-based topographic normalized backscattering coefficient γ^0, compared with the backscattering coefficient σ^0, for better tree volume estimation at stand level in mountain forests, KEF.

Results obtained from the linear regression between γ^0 and stand volume for the PALSAR images can lead to the estimation of tree volume on sloping terrain better than the linear regression between σ^0 and stand volume.

The advantage for using the γ^0 based on the topographic illumination correction model, proposed by Ulander [14], Castell *et al*. [2], and Zhou *et al*. [16], comes from correcting fore-slopes appearing brighter and far-slopes appearing darker in the PALSAR σ^0 images.

The potential for using the γ^0 for forest volume estimation associated with forest biomass evaluation using the PALSAR data seems to be promising. Future work will be also focused on the relationship between the fully polarimetric PALSAR (i.e., HH, VV, HV and VH) backscattering coefficients and the forest stand volume of mixed species forest.

REFERENCES

1. Beaudoin, A., Le Toan, T., Goze, S., Nezry, E., Lopes, A., Mougin, E., Hsu, C. C., Han, H. C., Long, J. A., and Shin, R. T., "Retrieval of forest biomass from SAR data," *International Journal of Remote Sensing*, Vol. 15, No. 14, pp. 2777-2796 (1994).
2. Castel, T., Beaudoin, A., Stach, N., Stussi, N., Le Toan, T., and Durand, P., "Sensitivity of space borne SAR data to forest parameters over sloping terrain," *International Journal of Remote Sensing*, Vol. 22, No. 12, pp. 2351-2376 (2001).
3. Dobson, M. C., Ulaby, F. T., Le Toan, T., Beaudoin, A., Kasischke, E. S., and Christensen, N., "Dependence of radar backscatter on coniferous forest biomass," *IEEE Transactions on Geoscience and Remote Sensing*, Vol. 30, No. 14, pp. 511-518 (1992).
4. Folkesson, K., Smith-Jonforsen, G., and Ulander, L. M. H., "Model-based compensation of topographic effects for improved stem-volume retrieval from CARABAS-II VHF-band SAR images," *IEEE Transactions on Geoscience and Remote Sensing*, Vol. 47, No. 4, pp. 1045-1055 (2009).
5. Jenet, M. A., Brendan, G., Kimberly, P., and Van, N., "Estimating forest biomass using satellite radar: an exploratory study in a temperate Austraian eucalyptus forest," *Forest Ecology and Management*, Vol. 176, pp. 575-583 (2003).
6. Kuplich, T., Salvatori, V., and Curran, P., "JERS-1/SAR back-scatter and its relationship with biomass of regenerating forests," *International Journal of Remote Sensing*, Vol. 21, pp. 2513-2518 (2000).
7. Longgéfé, N., Rakwatin, P., Isoguchi, O., Shimada, M., Uryo, Y., and Yulianto, K., "Assessment of ALOS PALSAR 50 m orthorectified FBD data for regional land cover classification by support vector machines,"

IEEE Transactions on Geoscience and Remote Sensing, Vol. 49, No. 6, pp. 2135-2150 (2011).

8. Lucas, R., Armston, J., Fairfax, R., Fensham, R., Accad, A., Carreiras, J., Kelly, J., Bunting, P., Clewley, D., Bray, S., Metcalfe, D., Dwyer, J., Bowen, M., Eyre, T., Laidlaw, M., and Shimada, M., "An evaluation of the ALOS PALSAR L-band backscatter-above ground biomass relationship Queensland, Australia : impacts of surface moisture condition and vegetation structure," *IEEE Journal of Selected Topics in Applied Earth Observations and Remote Sensing*, Vol. 3, No. 4, pp. 576-593 (2010).

9. Paloscia, S., Macelloni, G., Pampaloni, P., and Sigismondi, S., "The potential of C-band and L-band SAR in estimating vegetation biomass: the ERS-1 and JERS-1 experiments," *IEEE Transactions on Geoscience and Remote Sensing*, Vol. 37, pp. 2107-2110 (1999).

10. Santoro, M., Fransson, J. E. S., Eriksson, L. E. B., Magnusson, M., Ulander, L. M. H., and Olsson, H., "Signatures of ALOS PALSAR L-Band backscatter in Swedish forest," *IEEE Transactions on Geoscience and Remote Sensing*, Vol. 47, No. 12, pp. 4001-4019 (2009).

11. Shimada, M., "Orthorectification and slope correction of SAR data using DEM and its associated evaluation," *IEEE Journal of Selected Topics in Applied Earth Observations and Remote Sensing*, Vol. 3, No. 4, pp. 657-671 (2010).

12. Shimada, M., Isoguchi, O., Tadono, T., and Isono, K., "PALSAR radiometric and geometric calibration," *IEEE Transactions on Geoscience and Remote Sensing*, Vol. 49, No. 12, pp. 3915-3932 (2009).

13. Thiel, C. J., Thiel, C., and Schmullius, C. C., "Operational large-area forest monitoring in Siberia using ALOS PALSAR summer intensities and winter coherence," *IEEE Transactions on Geoscience and Remote Sensing*, Vol. 47, No. 12, pp. 3993-4000 (2009).

14. Ulander, L. M. H., "Radiometric slope correction of synthetic-aperture radar," *IEEE Transactions on Geoscience and Remote Sensing*, Vol. 34, No. 5, pp. 1115-1122 (1996).

15. Watanabe, M., Shimada, M., Rosenqvist, A., Tadono, T., Matsuoka, M., Romshoo, S. A., Ohta, K., Furuta, R., Nakamura, K., and Moriyama, T., "Forest structure dependency of the relation between L-band σ^0 and biophysical parameters," *IEEE Transactions on Geoscience and Remote Sensing*, Vol. 44, No. 11, pp. 3154-3165 (2006).

16. Zhou, Z. S., Lehman, E., Wu, X., Caccetta, P., McNeill, S., Mitchell, A., Milne, A., Tapley, I., and Lowell, K., "Terrain slope correction and precise registration of SAR data for forest mapping and monitoring," *Proceeding International Symposium Remote Sensing Environment*, pp. 1-4 (2011).